International Journal of Environmental Sciences
ISSN: 2229-7359
Vol. 11 No. 3S, 2025
https://www.theaspd.com/ijes.php

A Novel Enhancement Integrated Convolutional Neural Network for Automated Defect Detection in Photovoltaic Modules

Nitu Rana[1*] , Shaveta Arora[2]
[1] Research Scholar, Department of Multidisciplinary Engineering, The Northcap University, Gurugram, India
[1]Assistant Professor, Department of Electronics and Communication Engineering, Manav Rachna University, Faridabad, India
nitu19ecd004@ncuindia.edu, ernituchauhan@gmail.com
[2] Computer Science Engineering Department, The Northcap University, Gurugram, India
shavetaarora@ncuindia.edu
* corresponding author
Email: nitu19ecd004@ncuindia.edu

Abstract:
Due to ever-increasing demand of power globally, the focus is now shifted on renewable energy sources like hydro, wind, solar energy from non-renewable energy sources. Solar energy stands is a leading contributor in the sustainable energy revolution. The solar cells which are used to harness the solar energy suffer from several defects arising during the manufacturing or installation processes. Identifying these defects is crucial to prevent degradation in the performance of solar cells. However, manual detection is time consuming and tedious. Hence, automatic defect detection methods must be developed to improve efficiency. This paper proposes a novel image enhancement integrated Convolution Neural Network (IE-CNN) for defect detection in solar cells that involves pre-processing the input image through image enhancement and defect detection using CNN. The hyperparameters of the CNN are selected after extensive experimentation. The method converges fast and also takes care of the overfitting phenomenon. A dataset of electroluminescence (EL) images is used for the implementation of the proposed method. The proposed method achieved a precision of 0.97 and recall of 0.98, culminating in an elevated F1-score of 0.90.

Keywords- binary classification, deep learning, defect detection, electroluminescence images, solar cells

1. INTRODUCTION

The contribution of energy in the development of world's economy is significant. The rate at which the consumption of energy in the world is growing is huge. So many countries of the world have started looking for renewable sources of energy and solar energy is a major contributor for renewable energy sources.

The advancements and usage of solar energy is increasing at a fast pace and the total capacity of solar energy generated increased by 179 TWh in 2021 exhibiting a growth of 22% on 2020 according to the International Energy Agency. To achieve net zero emission by 2050 the average annual growth in generation must reach 25% for the period 2022-2030 [1].

An array of solar cells is the primary component for construction of Photovoltaic (PV) systems. The array of cells is encased in glass and housed within an aluminium frame, signifying the readiness of the PV system for installation. However, there are some factors like mechanical stress, thermal fluctuations, hailstorms, manufacturing defects, poor installation practices, corrosion, electrical overload, and exposure to certain chemicals or pollutants in the environment [2] which results into cracks or damage in the PV module cells[3][4]. This can reduce the efficiency of the entire system. Hence it is vital to find and replace damaged cells so that the efficiency of the PV System is maintained.

Visual identification of damaged cells in the PV module is not an easy and efficient method. When the cells are damaged in the module the temperature of the cell increases so Infrared (IR) imaging can be used to recognize those high temperature areas in a cell [5]. But a high temperature area may not be always a defect in an IR image. Therefore, using IR imaging for defect detection has its own limitations and may not be a good solution as mentioned by Ebner et al in[6]. It is also difficult to determine the precise region of the defect in IR images [7] and micro-cracks cannot be detected by IR images[8].

An alternative to IR imaging is electroluminescence (EL) imaging which can be used before installation of the PV module as well as after the installation to check the defects in the PV module [9].The EL images are extensively used by many researchers for defect identification in solar cells. Checking of PV cell EL images manually is a very tedious task and it is not possible to inspect the large solar farms manually. Therefore, automated defect detection methods are required to identify defective cells for further course of action [10].

The paper is structured as mentioned ahead: Section 2 gives a summary of the previous works. The methodology given in Section 3 covers the description of the dataset used along with in-depth discussion of the proposed approach. Section 4 outlines the experimental evaluation and results. Section 5 concludes the present work and lastly a comprehensive list of references is provided for further exploration.

2. RELATED WORKS

Deitsch et al. [5] introduced two distinct approaches to defect detection. The first approach relies on Support Vector Machine (SVM) and incorporates handcrafted features, while the second approach leverages Convolutional Neural Networks (CNN) for defect detection. There was limited discussion on potential challenges or limitations of the proposed method, which could impact the interpretation and practical implementation of the findings.

In [11] the authors used YOLO [12] for defect detection and ResNet18 [13] for defect classification. In [14] Akram et al. devised a CNN based method for detecting photovoltaic cell defects for improving solar energy system efficiency. They employed geometric transformations for data augmentation. The method had a limited generalizability to other defect types or imaging conditions. Due to reliance on biased training data, there is a risk of overfitting.

Tang et al. [15] in their work combined the generative adversarial network (GAN) based data augmentation with CNN architecture for identification of defects. The adaptability of the proposed technique to various defect types or image quality variations may be explored further.

Chunpeng et al., [16] presented a hybrid approach combining fuzzy logic and convolutional neural networks for accurate defect detection in photovoltaic cells, potentially enhancing quality control in solar panel manufacturing. With this Hybrid Fuzzy CNN, they were able to take care of the uncertainties in the PV cell data to improve the performance of their system. The complexity of the hybrid mechanism leads to high computational overhead and implementation challenges, potentially limiting its practical applicability in real-time defect detection systems.

In [17] the authors used Image Net pretrained ResNet101 as the backbone network and then bidirectional attention feature architecture was proposed which highlights the features of the defect and suppresses the background when performing the defect detection. Then they used a region proposal network to identify the region containing defect and mapped it to the matching level features of ResNet101.

The authors in [18] used contrast limited adaptive histogram equalization (CLAHE) for image enhancement and introduced a graph channel attention module for capturing pixel level interconnection in an image. Then they developed a light neural network using EfficientNet-B0 as the backbone network for defect detection.

Bartler et al. [19] introduced a CNN pipeline for defect detection and a balanced error rate (BER) of 7.73 % was achieved for binary classification. They also studied the effect of class imbalance in their work.

A high resolution deep learning network with a self-fusion network was introduced by the researchers in [20] for defect detection in PV modules. They also performed data augmentation prior to defect detection so as to create a balanced dataset.

The researchers in [21] proposed a CNN with eight convolutional and pooling layers followed by the dense layer for detection of dust on the solar panels. The scope of the CNN was limited to identifying dust on the panels and there is a scope for improving the capability of the architecture developed.

The research done in [22]involved feature extraction, selection and classification using a deep feature based support vector machine for binary and multiclass classification. The study done in [23] presented an investigation of YOLOv8 and enhanced YOLOv5 based model for automated defect detection. They integrated a Global Attention Module (GAM) with YOLOv5 to improve object representation. Further to improve feature fusion and model performance they incorporated an adaptive feature space fusion in the model.

2.1 Gaps identified

In summary, the literature review provides a thorough analysis of the defect detection methodologies. Despite the multitude of proposed approaches, certain persistent challenges are evident within the existing literature, such as concerns related to overfitting and the resource-intensive nature of hardware requirements. Additionally, there is a notable gap in addressing the application of image enhancement before CNN implementation. Furthermore, the prevalence of time-consuming and intricate methods emphasizes the necessity for more efficient and simplified approaches to be developed. Following are the gaps identified:

- Further exploration is required to investigate the integration of image enhancement techniques before implementing CNNs as including image enhancement in the proposed methods can lead to improved performance metrics.
- Complexity of hybrid mechanisms lead to increased computational overhead and implementation challenges like necessitating the use of GPUs and other specialized hardware accelerators.
- Training GANs requires momentous computational resources such as high-performance GPUs and huge memory expanses. Also training a GAN takes significant duration of time and it is expensive for high dimensional data.

2.2 Contribution

This study seeks to address these gaps through the integration of image enhancement techniques, the introduction of a tailored Convolutional Neural Network (CNN), and a meticulous comparative analysis. The insights gained from this review lay the foundation for advancing defect detection methodologies and contribute to the on-going evolution of automated defect detection systems. The experiments were performed within the Google Colab environment, showcasing its remarkable hardware resource efficiency for defect detection. Unlike previous efforts that placed limited emphasis on data pre-processing and image enhancement, this work makes notable contributions as given below:

- Implementation of image enhancement techniques, specifically contrast and brightness adjustments, applied to the images before the training process. After experimenting with different values, the final values are selected for image enhancement.
- The utilization of deep learning methodologies on the enhanced image dataset to detect defects, introducing a CNN based model designed specifically for defect detection.
- A comparison of this research with previous studies confirms the effectiveness of the proposed method. It also highlights advancements in defect detection achieved through improved pre-processing techniques and a customized CNN model.

3. METHODOLOGY

Within this section, we discuss the proposed framework, explaining its architecture and providing intricate details about the CNN employed. Figure 1 below displays the workflow of the proposed work.

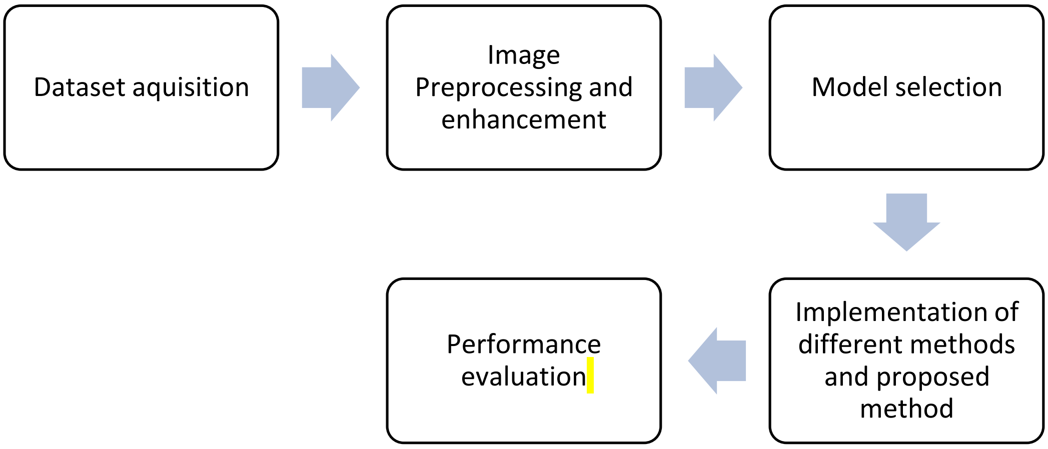

Figure 1 Workflow of the proposed work

3.1 Data Description

This research employed a dataset comprising of images categorized into two classes: defective and non-defective. Images from a publicly available dataset of EL images are used in this work [5] [24]. The source of these 2,624 EL images are 44 different PV modules and 18 modules are of monocrystalline and 26 are of polycrystalline type. The dimensions of the image are 300*300. Few images from the dataset are given in Figure 2 below.

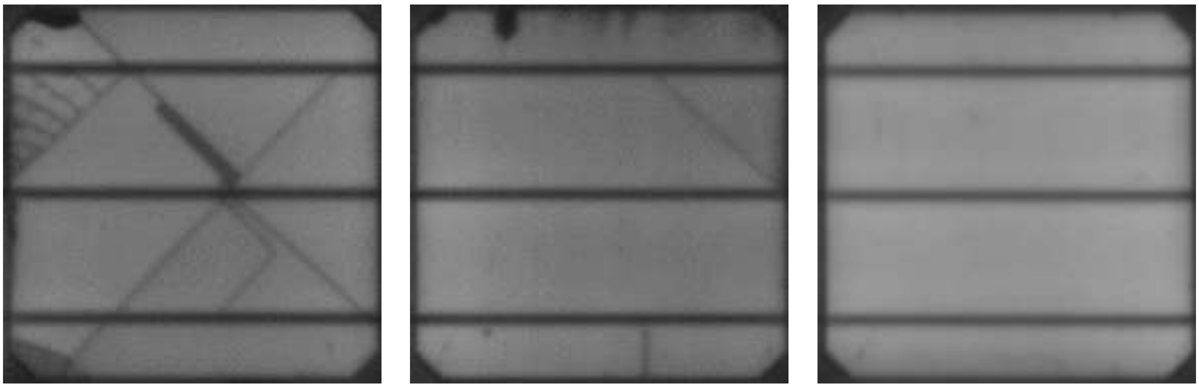

(a) (b) (c)

Figure 2 Sample images from the dataset [5] [24] (a) and (b) represent defective images (defect- crack) and (c) represents non-defective image

3.2 Image pre-processing and enhancement

The images are resized to 128×128 before applying the image enhancement operations to enhance their features for improved model training. Each image, denoted by I is pre-processed using image enhancement techniques before being fed into the CNN. The enhancement process involved applying a contrast adjustment function C (I, α) and a sharpness enhancement function S (I, β) to each image. The enhanced image I' is obtained as follows:

$$I' = S(C(I, \alpha), \beta) \quad (1)$$

where α and β are enhancement parameters controlling the degree of contrast adjustment and sharpness enhancement respectively. After experimenting with different values, the parameter α is set to 1.5, while β is assigned a value of 2.

Image enhancement prior to CNN implementation serves to improve the quality, consistency, and discriminative power of the input data, leading to more effective and reliable classification results. It helps the CNN extract meaningful features from the images, enhances model generalization, and leads to the overall success of the deep learning task.

To the best of our knowledge the potential benefits of pre-processing images with enhancement techniques has not been used previously and our work focuses specifically on integrating image enhancement into the proposed CNN. By refining the quality of images through contrast adjustment and sharpness enhancement, we aim to improve the quality and discriminative power of the input.

The application of contrast and sharpness enhancement using the specified factors resulted in noticeable improvements in image quality across the dataset. Visual comparisons and quantitative analysis demonstrated enhanced clarity, detail, and feature differentiation, which are essential for subsequent image analysis tasks such as object detection and classification.

3.3 Convolutional Neural Network Architecture

Our methodology involved thorough experimentation, where the images are pre-processed using enhancement techniques prior to training the proposed CNN model. After experimental evaluation it is deduced that the image enhanced CNN model outperforms previous approaches in terms of classification accuracy and other metrics. By highlighting the effectiveness of image enhancement in improving CNN performance, our research offers a sustainable advancement to the field of defect detection.

The convolutional neural network (CNN) architecture employed in this study is designed to identify the defective and non-defective images. The CNN consists of multiple layers, including convolutional, max-pooling, batch normalization, dropout, and fully connected layers.

3.3.1 Convolutional Layers

The first layer in our architecture is a convolutional layer CNN followed by max pooling and batch normalization. The role of convolution layer is to extract the low-level features from the enhanced input images. The convolutional layer applies a set of learnable filters to the input feature maps, generating output feature maps that capture spatial patterns in the images. Mathematically, the output feature map $Y^{(l)}$ of the l-th convolutional layer is computed as follows:

$$Y^{(l)} = ReLU(W^{(l)} * X^{(l-1)} + b^{(l)} \quad (2)$$

where $W^{(l)}$ represents the learnable weights (filters) of the l-th convolutional layer, $X^{(l-1)}$ denotes the input feature maps from the previous layer, $b^{(l)}$ is the bias, and $*$ signifies the convolution operation. The activation function used is ReLU. Each convolutional layer in the CNN is augmented with L2 regularization and a regularization term is added to the loss function. The regularization term penalizes the L2 norm of the weights, encouraging smaller weights and preventing overfitting. By incorporating L2 regularization into the methodology, we ensure that the CNN model is effectively regularized during training, leading to improved generalization performance and better handling of overfitting.

3.3.2 Batch Normalization

Batch normalization layers are inserted after each convolutional layer to normalize the activations, which helps stabilize and accelerate the training process.

$$\widehat{X}^{(l)} = \frac{X^{(l)} - \mu^{(l)}}{\sqrt{\sigma^{2(l)} + \epsilon}} \quad (3)$$

where $\widehat{X}^{(l)}$ represents the normalized activations, $\widehat{X}^{(l)}$ is the input activations, $\mu^{(l)}$ and $\sigma^{(l)}$are the mean and standard deviation of the batch, and ϵ is a constant of small value to get numerical stability.

3.3.3 Max-Pooling Layers

After each convolution layer there is a max-pooling layer to down sample the feature maps an reduce their spatial dimensions while retaining the important information. The max-pooling operation is defined as follows:

$$Y_{pooled}^{(l)}[i,j,k] = \max_{m,n} Y^{(l)}[2i+m, 2j+n, k] \quad (4)$$

where $Y_{pooled}^{(l)}$ denotes the output feature maps after max-pooling, $Y^{(l)}$ represents the input feature maps, and$[i,j,k]$ denote the spatial location and channel index.

3.3.4 Dropout Regularization

Dropout layers are added after certain convolutional layers to prevent overfitting by randomly dropping some of the neurons throughout training. The dropout operation is defined as follows:

$$Y_{dropout}^{(l)} = dropout(Y^{(l)}, p) \quad (5)$$

where $Y_{dropout}^{(l)}$ represents the output feature maps after dropout, $Y^{(l)}$ denotes the input feature maps, and p is the dropout probability.

3.3.5 Fully Connected Layers

The output of the convolutional layers is flattened and subsequently given to a series of fully connected layers and the classification is done on the extracted features. The fully connected layers in the CNN also incorporate L2 regularization to regulate the complexity of the model and improve its generalization performance. The output layer consists of two units with a sigmoid activation function, representing the probabilities of the input image fitting to each class.

3.4 Model Compilation and Training

The CNN model is compiled using categorical cross-entropy loss function and the Adamax optimizer. The compiled model is trained using a dataset containing pre-processed images and their corresponding labels. During training, model checkpoints and early stopping callbacks are employed to monitor the validation loss and prevent overfitting.

During training, the model's performance was evaluated based on accuracy metrics computed on a separate validation set. The training process aimed to minimize the categorical cross-entropy loss while maximizing classification accuracy. Additionally, model hyper parameters such as learning rate, dropout rates, and regularization parameters are fine-tuned through iterative experimentation to achieve optimal performance. Training hyper parameters of the proposed architecture are given in Table 1.

Table 1. Training hyper parameters

Parameter	Value
Backbone architecture	Custom
Classes	Two
Batch size	32
Epochs	150
Image size	128x128x1
Kernel regularizer (l2)	0.02
Optimiser	Adamax
Loss	categorical cross entropy
Activation function	Relu (input and hidden layers), Sigmoid (output layer)
Environment	Python 3, T4 GPU on Google Colab

After examining the dataset which consists of both monocrystalline and poly crystalline PV cells it is noticed that in images labelled as defective with 33% probability or 66 %, it is difficult to make out whether it is defective or not. Also, the homogeneous surface of mono crystalline cells is different from the background surface of polycrystalline cells. This makes it difficult to detect the defects. The image dataset is pre-processed and a set of architectures are explored as shown in Figure 3.

After studying few previous works and experimenting with different hyper parameters image enhancement integrated CNN is proposed. Different CNN models are implemented before finalizing the model. The architectures implemented are given in Figure 3(a), (b) and (c).

In the proposed model 1 there is an input layer, two hidden layers and one output layer as shown in Figure 3(a). The model exhibits poor performance and overfitting. To overcome the effect of overfitting and low performance of the model an additional hidden layer is added to the model 2.

Further overfitting is handled by adding kernel regularization to the model. L2 kernel regularizer with L2=0.2 is added to the hidden layers and output layer to improve the performance of the model. By increasing the number of convolution layers the model performance is also increasing. But adding more layers will increase the model complexity and it will also make the model computationally expensive. Among Model 1, Model 2, and Model 3, Model 3 demonstrates superior performance compared to the others. To enhance the model's performance further, image enhancement techniques are employed prior to inputting them into the CNN. This involved improving the contrast and brightness of the images before training the CNN architecture proposed in Model 3.

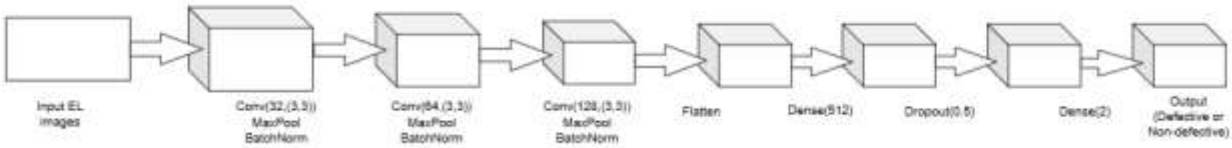

(a)

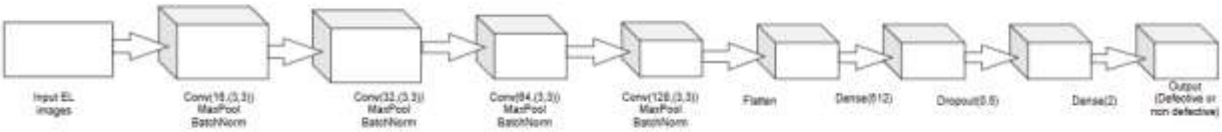

(b)

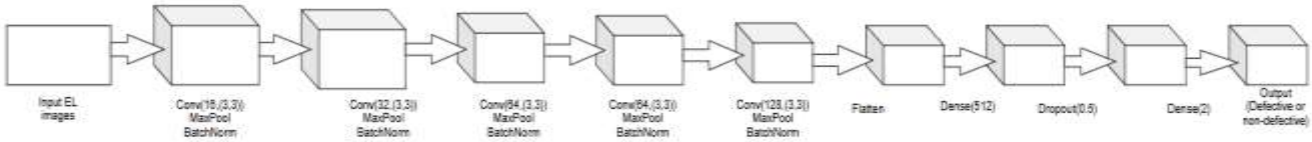

(c)

Figure 3 (a) Proposed model 1 (b) Proposed model 2 (c) Proposed model 3

4. EXPERIMENTAL EVALUATION

4.1 Performance evaluation

The performance metrics accuracy, precision, recall and F1 score are used to evaluate the model [25].

(i) Accuracy: It represents the ratio of correctly predicted instances to the total instances in the dataset and is computed as the ratio of number of correct predictions to the total number of predictions. However, the accuracy provides an overall measure of model performance but it may not be most informative metric in cases of imbalanced datasets.

(ii) Precision: It quantifies the accuracy of positive predictions, measuring the ratio of correctly predicted positive observations to the total predicted positives. Precision is crucial when the cost of false positives is high. It helps in assessing the capability of the model to check false alarms.

(iii) Recall: It gauges the model's ability to identify all relevant instances, measuring the ratio of correctly predicted positive observations to the actual positives in the dataset. Recall is important when the cost of false negatives is high. It reflects the model's sensitivity in capturing all instances of the positive class.

(iv) F1 score: It integrates precision and recall into a single value and is particularly useful in case of an uneven class distribution (class imbalance). The F1 score is calculated using the harmonic mean of precision and recall, providing a balanced measure of a model's performance.

The F1 score, ranging from 0 to 1, is a valuable metric for defect detection, especially when striking a balance between precision and recall is crucial. Its sensitivity to both false positives and false negatives, weighted by the harmonic mean, makes it well-suited for tasks requiring a comprehensive evaluation. In defect detection scenarios, where achieving a balance between precision and recall is often sought, the F1 score helps prevent scenarios where a model excels in one aspect but falters in the other. This metric aids in making informed decisions about the trade-off between precision and recall, catering to the specific requirements of the application, such as prioritizing high precision in quality control or emphasizing high recall in medical diagnoses. Analysing these metrics collectively provides a nuanced understanding of a model's performance, guiding informed deployment decisions[26].

4.2 Results and Discussions

An analysis and comparison of the proposed methods and other deep learning methods is presented in this section. Simple MNIST Convnet [13], CNN for defect detection [5], and three different architectures proposed are implemented on the benchmark elpv dataset [10, 11] for defect detection. Precision, recall, F1 score and accuracy metrics are computed and given in Table 2 to compare the performance of all the methods.

The CNN architecture used in [15] has two convolution layers and one fully connected layer which is suitable for the MNIST dataset but for elpv dataset a network with a greater number of layers will be suitable as the size of images is large as compared to the MNIST dataset images. In [8] the network has four convolution layers and two fully connected layers. Both the architectures have used Adam optimizer. In [8] dropout is used in output layer only.

The evaluation of several models on the MNIST dataset reveals insightful findings regarding their classification performance. Among the tested models, the MNIST Convnet and Convolution Neural Network [8] demonstrate respectable precision scores of 0.81, although with varying levels of recall and F1-scores. Model 1, while achieving a slightly lower precision of 0.75, maintains a comparable accuracy of 0.75. Notably, Model 2 exhibits notable improvements in precision, recall, and F1-score, boasting values of 0.83, 0.81, and 0.82, respectively, resulting in an accuracy of 0.85. Interestingly, our proposed Model 3 maintains a similar precision to Model 2 but shows a slight reduction in recall, yet maintains a commendable F1-score of 0.73 and an accuracy of 0.80. However, the most striking improvement is observed in Model 3 with image enhancement, achieving an impressive precision of 0.97 and recall of 0.98, culminating in an elevated F1-score of 0.90 and accuracy of 0.87. These results underscore the potential of image enhancement techniques in enhancing the performance of CNN. Figures 4, 5, and 6 illustrate the loss and accuracy curves for models 1, 2, and 3, respectively.

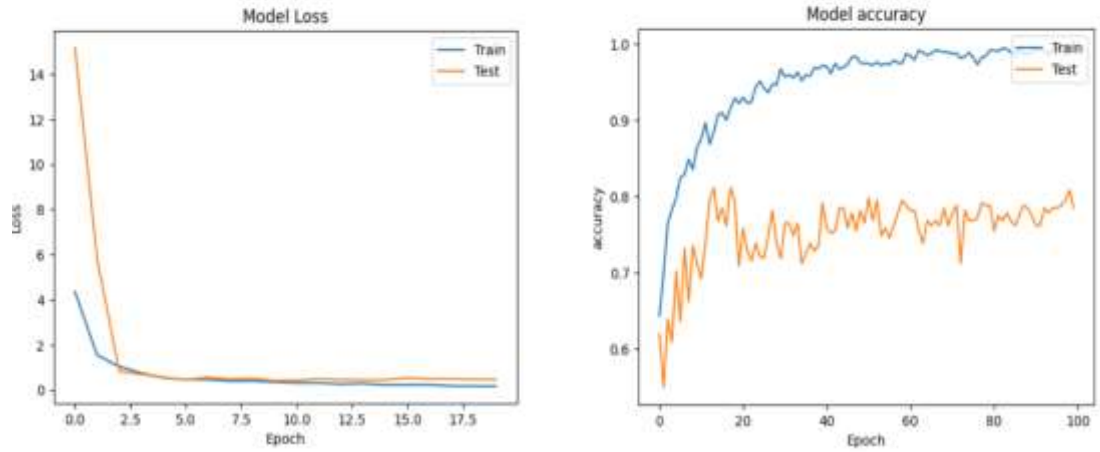

Figure 4 Loss and accuracy curve of model 1

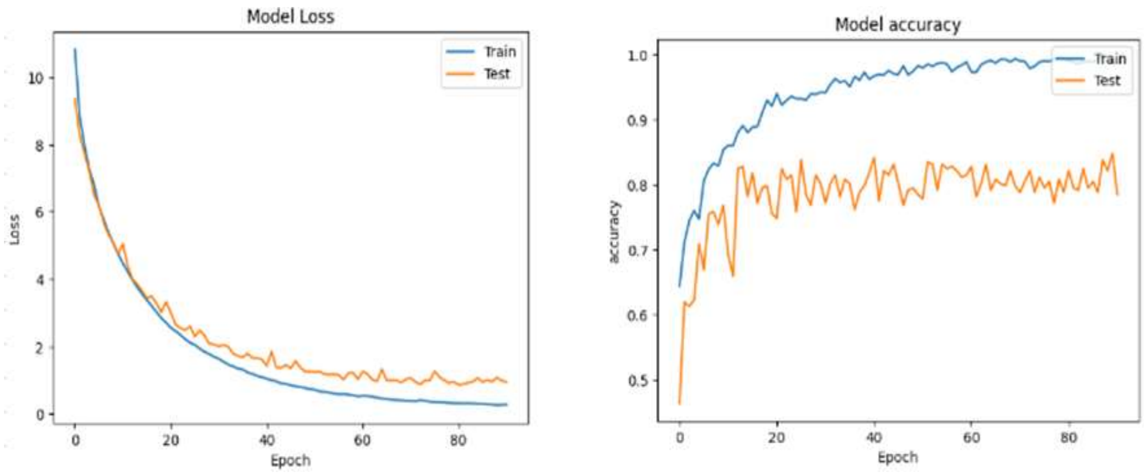

Figure 5 Loss and accuracy curve of model 2

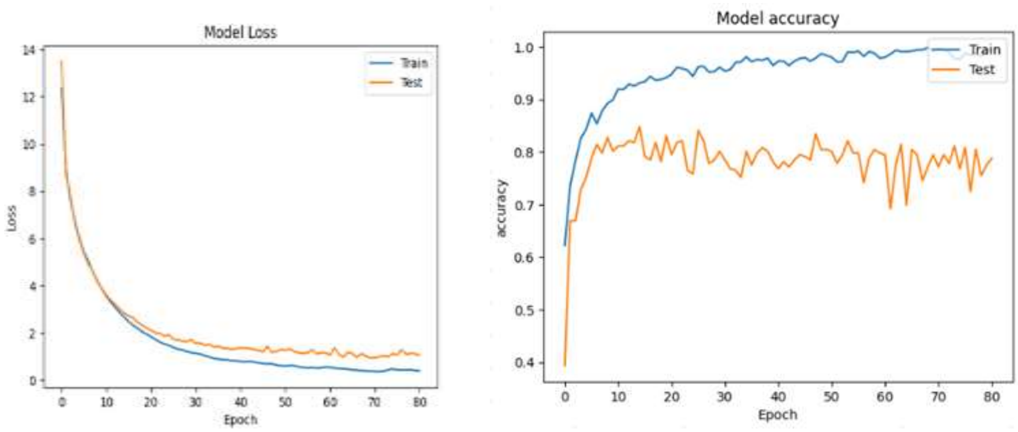

Figure 6 Loss and accuracy curve of model 3

Table 2. Precision, Recall and F-1 score of proposed models with the existing methods on the ELPV dataset

Method	Precision	Recall	F1-score	Accuracy
CNN [27]	0.81	0.67	0.73	0.80
CNN [14]	0.81	0.60	0.69	0.78
Model 1	0.75	0.59	0.66	0.75
Model 2	0.83	0.81	0.82	0.85
Model 3 (Proposed model)	0.83	0.66	0.73	0.80
Model 3 (Proposed model) with image enhancement-IE-CNN	**0.97**	**0.98**	**0.90**	**0.87**

5. CONCLUSIONS

The proposed approach introduces a novel pipeline where an image enhancement method and a deep learning-based method are integrated to distinguish between defective and non-defective photovoltaic (PV) cells. The results are also given to validate the effectiveness of the method. A notable challenge arises from the dataset's inclusion of both monocrystalline and polycrystalline PV cells, each with distinct backgrounds, complicating defect identification. In this research, attention is given to optimizing hyper parameters such as optimizers, loss functions, and regularizers to achieve optimal performance. The advantage of the suggested architecture is its simplicity and hardware efficiency leading to a sustainable solution for maintaining the performance of the PV modules. Additionally, enhanced results can be attained by implementing data augmentation techniques and ensemble learning. Exploring hybrid methods, such as those described in[16] , offers a probable avenue for further refining the automatic defect detection process.

6. REFERENCES

[1] International Energy Agency - IEA, "Electricity 2024 Analysis and forecast to 2026.," *Int. Energy Agency*, pp. 1–170, 2023, [Online]. Available: https://www.iea.org/news/global-coal-demand-expected-to-decline-in-coming-years

[2] R. J. Mustafa, M. R. Gomaa, M. Al-Dhaifallah, and H. Rezk, "Environmental impacts on the performance of solar photovoltaic systems," *Sustain.*, vol. 12, no. 2, Jan. 2020, doi: 10.3390/su12020608.

[3] M. Aghaei, A. Gandelli, F. Grimaccia, S. Leva, R. E. Zich, and P. Di Milano, "IR real-time Analyses for PV system monitoring by Digital Image Processing Techniques."

[4] S. R. Madeti and S. N. Singh, "Monitoring system for photovoltaic plants: A review," *Renew. Sustain. Energy Rev.*, vol. 67, pp. 1180–1207, 2017, doi: 10.1016/j.rser.2016.09.088.

[5] S. Deitsch *et al.*, "Automatic Classification of Defective Photovoltaic Module Cells in Electroluminescence Images," Jul. 2018, doi: 10.1016/j.solener.2019.02.067.

[6] R. Ebner, S. Zamini, and G. Újvári, "Defect Analysis in Different Photovoltaic Modules Using Electroluminescence (EL) and Infrared (IR)-Thermography," 2010, doi: 10.4229/25thEUPVSEC2010-1DV.2.8.

[7] I. Energy, A. Photovoltaic, P. Systems, I. E. Agency, P. Version, and D. On, *Review on infrared and electroluminescence imaging for PV field applications : International Energy Agency Photovoltaic Power Systems Programme Review on Infrared and Electroluminescence Imaging for PV Field Applications*. 2018.

[8] U. Jahn *et al.*, *Review on Infrared and Electroluminescence Imaging for PV Field Applications*. 2018.

[9] T. Berghout, M. Benbouzid, T. Bentrcia, X. Ma, and S. Djurovi, "Machine Learning-Based Condition Monitoring for PV Systems : State of the Art and Future Prospects," pp. 1–24, 2025.

[10] R. Sensing *et al.*, "DEEP CONVOLUTIONAL NEURAL NETWORK FOR AUTOMATIC DETECTION OF DAMAGED PHOTOVOLTAIC CELLS," vol. XLII, no. June 2018, pp. 4–7, 2020.

[11] X. Chen, T. Karin, and A. Jain, "Automated defect identification in electroluminescence images of solar modules," *Sol. Energy*, vol. 242, pp. 20–29, 2022, doi: 10.1016/j.solener.2022.06.031.

[12] G. Plastiras, C. Kyrkou, and T. Theocharides, "Efficient convnet-based object detection for unmanned aerial vehicles by selective tile processing," *ACM Int. Conf. Proceeding Ser.*, 2018, doi: 10.1145/3243394.3243692.

[13] T. Hattiya, K. Dittakan, and S. Musikasuwan, "Diabetic Retinopathy Detection using Convolutional Neural Network: A Comparative Study on Different Architectures," *Eng. Access*, vol. 7, no. 1, pp. 50–60, 2021, doi: 10.14456/mijet.2021.8.

[14] M. W. Akram *et al.*, "CNN based automatic detection of photovoltaic cell defects in electroluminescence images," *Energy*, vol. 189, Dec. 2019, doi: 10.1016/j.energy.2019.116319.

[15] W. Tang, Q. Yang, K. Xiong, and W. Yan, "Deep learning based automatic defect identification of photovoltaic module using electroluminescence images," *Sol. Energy*, vol. 201, pp. 453–460, May 2020, doi: 10.1016/j.solener.2020.03.049.

[16] C. Ge, Z. Liu, L. Fang, H. Ling, A. Zhang, and C. Yin, "A Hybrid Fuzzy Convolutional Neural Network Based Mechanism for Photovoltaic Cell Defect Detection with Electroluminescence Images," *IEEE Trans. Parallel Distrib. Syst.*, vol. 32, no. 7, pp. 1653–1664, Jul. 2021, doi: 10.1109/TPDS.2020.3046018.

[17] B. Su, H. Chen, and Z. Zhou, "BAF-Detector : An Efficient CNN-Based Detector for Photovoltaic Cell Defect Detection," vol. 0046, no. c, 2021, doi: 10.1109/TIE.2021.3070507.

[18] Q. Liu, M. Liu, C. Wang, and Q. M. J. Wu, "An efficient CNN-based detector for photovoltaic module cells defect detection in electroluminescence images," *Sol. Energy*, vol. 267, no. September 2023, p. 112245, 2024, doi: 10.1016/j.solener.2023.112245.

[19] Università degli studi Roma tre, European Association for Signal Processing, IEEE Signal Processing Society, and Institute of Electrical and Electronics Engineers, *EUSIPCO 2018 : 26th European Signal Processing Conference : Rome, Italy, September 3 - 7, 2018*.

[20] X. Zhao, C. Song, H. Zhang, X. Sun, and J. Zhao, "HRNet-based automatic identification of photovoltaic module defects using electroluminescence images," *Energy*, vol. 267, no. March, pp. 1–8, 2023, doi: 10.1016/j.energy.2022.126605.

[21] M. S. H. Onim *et al.*, "SolNet: A Convolutional Neural Network for Detecting Dust on Solar Panels," *Energies*, vol. 16, no. 1, Jan. 2023, doi: 10.3390/en16010155.

[22] M. Y. Demirci, N. Beşli, and A. Gümüşçü, "Efficient deep feature extraction and classification for identifying defective photovoltaic module cells in Electroluminescence images," *Expert Syst. Appl.*, vol. 175, no. February, 2021, doi: 10.1016/j.eswa.2021.114810.

[23] F. M. A. Mazen, R. A. A. Seoud, and Y. O. Shaker, "Deep Learning for Automatic Defect Detection in PV Modules Using Electroluminescence Images," *IEEE Access*, vol. 11, no. June, pp. 57783–57795, 2023, doi: 10.1109/ACCESS.2023.3284043.

[24] S. D. C. Buerhop-lutz *et al.*, "Segmentation of photovoltaic module cells in uncalibrated electroluminescence images," *Mach. Vis. Appl.*, vol. 32, no. 4, pp. 1–23, 2021, doi: 10.1007/s00138-021-01191-9.

[25] D. Berrar, "Performance measures for binary classification," *Encycl. Bioinforma. Comput. Biol. ABC Bioinforma.*, vol. 1–3, pp. 546–560, 2018, doi: 10.1016/B978-0-12-809633-8.20351-8.

[26] S. Sagiroglu, T. T. Temizel, and N. Baykal, "Binary Classification Performance Measures / Metrics :," 2017.

[27] W. Tang, Q. Yang, and W. Yan, "Deep Learning-Based Algorithm for Multi-Type Defects Detection in Solar Cells with Aerial EL Images for Photovoltaic Plants," *C. - Comput. Model. Eng. Sci.*, vol. 130, no. 3, pp. 1423–1439, 2022, doi: 10.32604/cmes.2022.018313.